Investigation of Ion Transport in Network Polymers from Poly(propylene oxide) Using Azobenzene Probes

Masayoshi Watanabe,* Akiko Suzuki, Tsuyoshi Santo, Kohei Sanui, and Naoya Ogata

Department of Chemistry, Sophia University, Chiyoda-ku, Tokyo 102, Japan.

Received August 23, 1985

ABSTRACT: Azobenzene chromophores were incorporated into network polymers from poly(propylene oxide) (PPO) containing lithium perchlorate ($LiClO_4$). Ionic conductivity, thermal cis → trans isomerization rate of the azochromophores, and dielectric relaxation time for the backbone motion were studied for the salt-free network polymers and the PPO–$LiClO_4$ complexes in the rubbery state. The ionic conductivity of the PPO–$LiClO_4$ complexes showed a Williams–Landel–Ferry (WLF) type temperature profile and was influenced by the increase in glass transition temperature (T_g) due to the increase in both $LiClO_4$ concentration and cross-linking density. The temperature dependence of the dielectric relaxation time also showed WLF behavior, and its magnitude increased with increasing cross-linking density. In contrast, the thermal isomerization rate of the azochromophores in the salt-free network polymers and the PPO–$LiClO_4$ complexes, which obeyed first-order kinetics, was hardly changed by the increase in T_g due to the increase in both $LiClO_4$ concentration and cross-linking density. The temperature dependence of the isomerization rate was expressed by a single Arrhenius equation with an activation energy of 0.96 eV, which agreed with that of many low molecular weight azobenzene derivatives in dilute solutions. These results suggest that the average hole size in the matrix was larger than the average hole size required to allow the thermal isomerization and smaller than the average hole size for the ionic transport. The backbone motion with the associated carrier ions may be the rate-determining step for the ionic conduction.

Introduction

High ionic conductivity in certain kinds of ion-containing polymers has been the subject of a number of recent studies.[1-11] Polymers having both a high concentration of polar groups and a low glass transition temperature (T_g), such as poly(ethylene oxide),[1-3] poly(propylene oxide) (PPO),[3-6] poly(β-propiolactone),[7] poly(ethylene succinate),[8,9] polyphosphazene,[10] poly(ethylene oxide-*co*-dimethylsiloxane),[11] and poly(ethylenimine),[12] have been selected as host polymers for salts, especially for alkali metal salts. Up to now, T_gs of the polymer complexes with high ionic conductivities lie below the temperature range for the conductivity measurements. As a result, it has been pointed out by several authors that the temperature dependence of ionic conductivity does not obey the Arrheniuus equation, but obeys the Vogel–Tamman–Fulcher equation[1] or the Williams–Landel–Ferry (WLF) equation.[3-6] These two equations can be derived from free volume theory. Thus, ion transport in these polymer complexes strongly depends on the probability of redistribution of the free volume, which is large enough to allow ionic migration.

It has been reported that the ratio of the conductivity at a given temperature ($>T_g$) to that at T_g is roughly in proportion to the shift factor of the dielectric relaxation time or the mechanical relaxation time for some insulating polymers[13,14] and for the polyether networks containing salts.[3] The proportionality constant is considered to be the ratio of the minimum hole size required to allow ionic migration to that required to allow the motion of the elementary unit of the polymer chain involved in the relaxation process.[3,13]

In this study, ion transport in network polymers from PPO containing lithium perchlorate ($LiClO_4$) was investigated. Azobenzene chromophores were used as a cross-linking reagent and were incorporated into the PPO networks in order to gain an insight into the ion-transport process. The ionic conductivity, the thermal cis → trans isomerization rate of the chromophores, and the dielectric relaxation time for the backbone motion were measured for the salt-free network polymers and the PPO–$LiClO_4$ complexes. From a comparison of the temperature dependences of these three values, the ion-transport process was discussed.

Experimental Section

Materials. Triol-type PPOs with number-average molecular weights of 750 (PPO-700) and 420 (PPO-400) were supplied from Asahi Denka Kogyo Co. and dried under reduced pressure at 80 °C for 8 h before use. 4,4′-Azobenzoxyl chloride was synthesized according to the literature.[15] The crude products were recrystallized several times from ligroin: mp 168 °C (164 °C[15]); IR (KBr disk): 3090 (w), 1780 (s), 1735 (m), 1200 (s), 880 cm^{-1} (s); NMR ($CDCl_3$): δ 7.94–8.31 (8 H, m, phenylene protons). Anal. Calcd for $C_{14}H_8N_2O_2Cl_2$ (307.14): C, 54.7; H, 2.63; N, 9.12. Found: C, 54.6; H, 2.6; N, 9.1. A special grade anhydrous $LiClO_4$ (Mitsuwa Kagaku Co.) was dried under reduced pressure (10^{-3} torr) at 180 °C for 8 h. The other reagents and solvents were purified by conventional methods.

PPO network films were prepared by a cross-linking reaction of triol-type PPO with 4,4′-azobenzoxyl chloride and sebacoyl chloride, as shown in Figure 1. With respect to the functional groups, stoichiometric amounts of PPO, 4,4′-azobenzoxyl chloride, and sebacoyl chloride were weighed, and dissolved in chlorobenzene. Total precursor concentration in the solution was 50–60 wt %. A weight fraction of 4,4′-azobenzoxyl chloride in the precursors of 0.011–0.013 kept the optical density (330 nm) of the resulting films at about 1.5. The solution was mixed under nitrogen atmosphere at room temperature for 5 min and cast on a glass substrate. The cross-linking reaction proceeded at 40 °C for 24 h under a nitrogen atmosphere and at 80 °C for 48 h under vacuum. Low molecular weight substances in the network polymers were extracted with acetone several times. The network films were dried again under vacuum at 80 °C for 48 h. Thickness of the network films was 0.3–0.5 mm. The network films obtained had a single phase structure and were completely amorphous.

The dissolution of $LiClO_4$ in the network polymers was performed by an immersion method, as described elsewhere.[4] The concentration of $LiClO_4$ in the network films was determined from the weight change of the film before and after immersion and was represented by the molar ratio of $LiClO_4$ to the repeat unit of PPO ($[LiClO_4]/[PO\ unit]$). Thermal and X-ray analyses revealed that the PPO–$LiClO_4$ complexes obtained also had a single-phase structure and were completely amorphous in the $LiClO_4$ concentration range investigated in this study.

Handling of the PPO network polymers and the PPO–$LiClO_4$ complexes was all carried out under inert atmosphere within an argon-filled drybox in order to exclude traces of water.

0024-9297/86/2219-1921$01.50/0

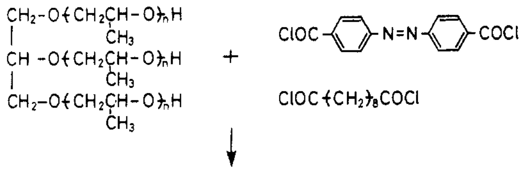

Figure 1. Preparation of PPO network polymers.

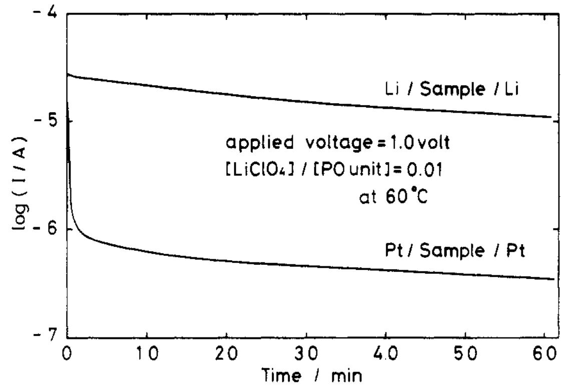

Figure 2. Time dependence of current through PPO-700–$LiClO_4$ complex ($[LiClO_4]/[PO\ unit] = 0.01$) with platinum or lithium electrodes under a step voltage of 1.0 V.

Methods. The PPO network films and the PPO–$LiClO_4$ complexes, which were cut into disks of 13-mm diameter, were sandwiched between electrodes (13-mm diameter) and packed in a sealed cell under an argon atmosphere within the drybox. Platinum was used as an electrode material unless otherwise noted. These cells were used for electrical measurements. Ionic conductivity of the PPO–$LiClO_4$ complexes was determined from the complex impedance measurements.[4,9] The frequency dependence of the cell impedance was measured with a Yokogawa-Hewlett-Packard 4192A LF-impedance analyzer. The frequency dependence of the dielectric constant and dissipation factor for the PPO network films was measured by using the impedance analyzer, assuming that an equivalent circuit of the cell was expressed by the parallel combination of capacity and resistance.

Thermal cis → trans isomerization rates of the azochromophores were determined spectroscopically. The PPO network films and the PPO–$LiClO_4$ complexes (9 mm × 35 mm) were attached to the inside of a quartz cell within the drybox. The cell was tightly sealed in the drybox. UV light of constant intensity was directed at the samples through a Toshiba UV-D36C glass filter from an Ushio 501C 250-W super-high-pressure mercury lamp at room temperature. After the sample reached a photo steady state, the cell was left in the dark at a given temperature, and UV-vis spectra were measured periodically with a Shimazu UV-240 spectrophotometer.

Differential scanning calorimetry (DSC) was carried out by using a Rigaku Denki 8058 DSC apparatus over the temperature range of −160 to 200 °C at a heating rate of 20 °C min^{-1}. T_g was defined as the midpoint of the heat capacity change during the glass transition.

Results and Discussion

Ionic Conductivity. Figure 2 shows the time dependence of the current through the PPO-700–$LiClO_4$ complex ($[LiClO_4]/[PO\ unit] = 0.01$) with platinum or lithium electrodes under a step voltage of 1.0 V. The current through the platinum electrode cell decreased rapidly within an initial few minutes and continued to decrease gradually for a prolonged period, whereas the current through the lithium electrode cell decreased slightly in this period. The current level at 60 min was higher in the lithium electrode cell by 1.5 orders of magnitude. Platinum is a nonblocking electrode toward electrons but a blocking electrode toward ions (Li^+ and ClO_4^- ions). Lithium is an ion-reversible electrode toward Li^+ ions. Thus, this result suggested that the PPO–$LiClO_4$ complex was primarily an ionic conductor.

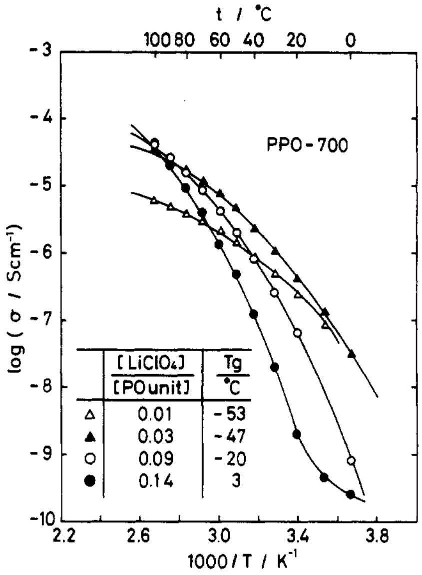

Figure 3. Temperature dependence of ionic conductivity for PPO-700–$LiClO_4$ complexes.

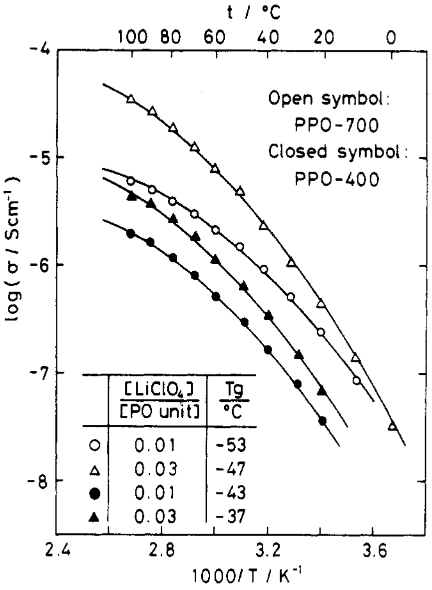

Figure 4. Temperature dependence of ionic conductivity for PPO-700–$LiClO_4$ and PPO-400–$LiClO_4$ complexes.

Figure 3 shows the temperature dependence of the ionic conductivity for the PPO-700–$LiClO_4$ complexes. As shown in the figure, the T_gs of the samples increased considerably with increasing $LiClO_4$ concentration. The temperature dependence deviated positively from straight lines and showed the so-called WLF-type profile. The ionic conductivity at a given temperature tended to increase with increasing $LiClO_4$ concentration up to 0.03 but tended to decrease for higher concentrations. The ionic conductivity is determined by the product of the number of carrier ions and their mobility. The decrease in the conductivity may be mainly attributed to the decrease in the carrier mobility, owing to the increase in T_g. Thus, it is clear that the ion transport in the PPO networks is related to the segmental motion of the matrix polymer. The segmental motion of the PPO networks could also be changed by the change in the cross-linking density. The effect of the cross-linking density on the ionic conductivity was investigated at the same $LiClO_4$ concentrations, as shown in Figure 4. The T_gs of the PPO-400–$LiClO_4$

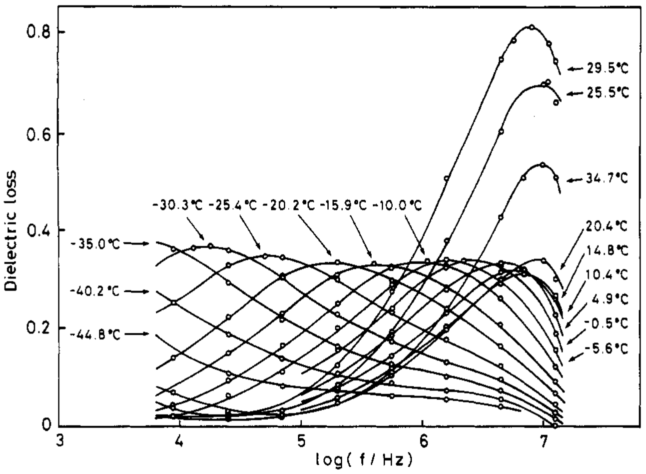

Figure 5. Frequency dependence of dielectric loss for PPO-700 network polymer at various temperatures.

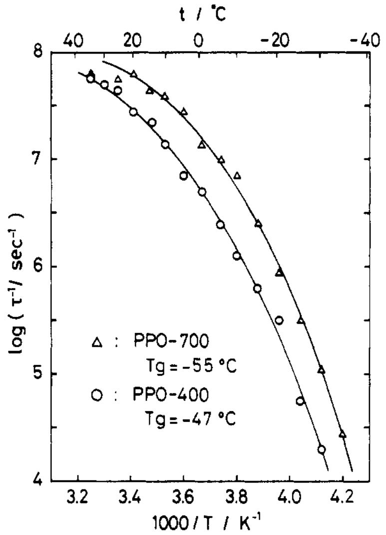

Figure 6. Reciprocal of dielectric relaxation time plotted against $1/T$ for PPO-700 and PPO-400 network polymers.

complexes were higher than those of the PPO-700–$LiClO_4$ complexes by 10 °C at the same concentrations. The ionic conductivity of the PPO-400–$LiClO_4$ complexes was lower than that of the PPO-700–$LiClO_4$ complexes, reflecting the higher T_gs of the PPO-400–$LiClO_4$ complexes.

Dielectric Relaxation. Figure 5 shows the frequency dependence of the dielectric loss for the PPO-700 network at various temperatures. The relaxation frequencies shifted to the higher frequency side with increasing temperature. The reciprocal of the dielectric relaxation time (τ) was plotted against $1/T$ for the PPO-700 and PPO-400 network polymers, as shown in Figure 6. The temperature dependence of τ^{-1} showed a WLF-type profile, indicating that these relaxation processes can be assigned to the backbone motion of the network polymers. The τ^{-1} values were smaller for the PPO-400 network at the same temperatures. The result had some analogy with the result of Figure 4; i.e., both τ^{-1} value and ionic conductivity decreased with increasing cross-linking density.

Thermal Cis → Trans Isomerization. The azochromophores in the PPO network polymers and the PPO–$LiClO_4$ complexes underwent reversibly trans → cis isomerization by the UV light irradiation and cis → trans isomerization by visible light irradiation (>390 nm). When the samples that reached a photo steady state by the UV light irradiation were left in the dark, the chromophores underwent thermal cis → trans isomerization. Figure 7 shows the change in the spectra with time for the PPO-700–$LiClO_4$ complex ($[LiClO_4]/[PO\ unit] = 0.09$) after reaching the photo steady state and being left in the dark at 35 °C. The absorption at 330 nm, assignable to the π–π^* transition of the trans form, increased with time, whereas the absorptions near 440 and 260 nm, assignable to the n–π^* and cis π–π^* transitions, respectively, decreased with time. Kinetics of the thermal isomerization were studied, assuming that the absorption of the cis form at 330 nm was negligible. The absorbance of 330 nm at a given time (A_T) is assumed to obey the following equation based on first-order kinetics

$$(A_\infty - A_T) = (A_\infty - A_0)\exp(-kt) \tag{1}$$

where A_∞ is the absorbance at infinite time, which is assumed to be equal to the absorbance before the UV light irradiation, A_0 is the absorbance at the photo steady state, and k is the rate constant. At the photo steady state, 60% of the azochromophores were in the cis form. Figure 8 shows the first-order plots for the PPO-700 network polymer at various temperatures. The thermal isomerization kinetics were expressed reasonably by eq 1.

The Arrhenius plots of the rate constant for the PPO-700 network polymer and the PPO-700–$LiClO_4$ complexes are shown in Figure 9. The temperature dependence of the rate constant was expressed by a single straight line and was insensitive to the large increase in T_g accompanied by the increase in $LiClO_4$ concentration. This result contrasts with the conductivity result shown in Figure 3. Figure 10 shows the Arrhenius plots of the

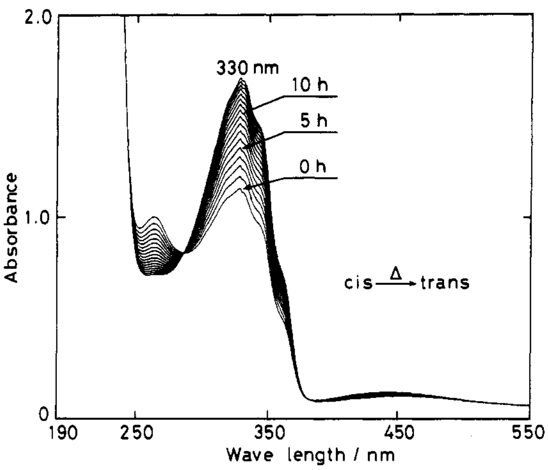

Figure 7. Change in UV–vis spectra with time for PPO-700–$LiClO_4$ complex ($[LiClO_4]/[PO\ unit] = 0.09$) after reaching a photo steady state by UV irradiation and being left in the dark at 35 °C.

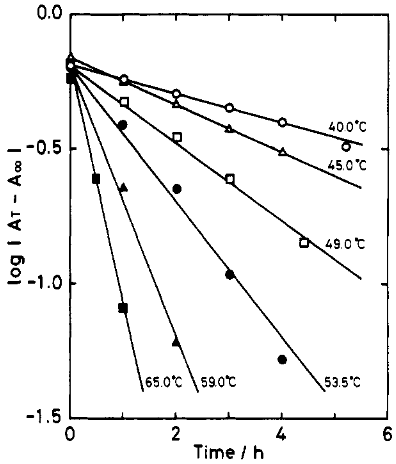

Figure 8. First-order plots of thermal cis → trans isomerization for PPO-700 network polymer at various temperatures.

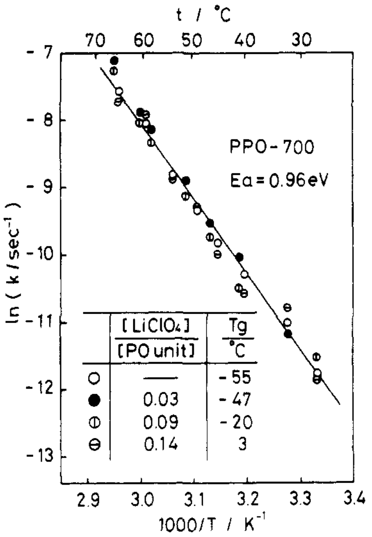

Figure 9. Arrhenius plots of thermal cis → trans isomerization rate for PPO-700 network polymer and PPO-700–$LiClO_4$ complexes.

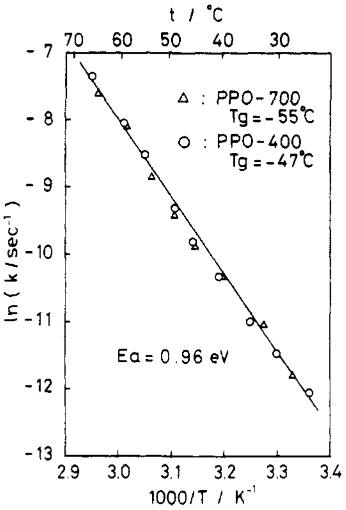

Figure 10. Arrhenius plots of thermal cis → trans isomerization rate for PPO-700 and PPO-400 network polymers.

rate constant for the PPO-700 and PPO-400 network polymers. The temperature dependence was also expressed by the same linear line. This result contrasts with the results of both ionic conductivity and dielectric relaxation time, shown in Figures 4 and 6, respectively. The activation energy for the thermal isomerization was 0.96 eV. The rate constant of the monomer analogue (azobenzoxyl chloride) in a *n*-hexane solution was only 5 times as large as that of the films at room temperature. The activation energy obtained for the films also agreed with that of various azobenzene derivatives in dilute solutions.[16] Recent work by Lamarre and Sung[17] showed that the thermal isomerization rate of azo labels in the main chains of the amorphous polyurethanes was slightly lower in the rubbery matrix than in dilute solution. However, the activation energies (15–18 kcal/mol) were quite similar for both states. Our results are consistent with their results.

The thermal isomerization of azochromophores seems to proceed when the chromophores have around them a free volume that is larger than the critical hole size required for the isomerization. The frequency factor of the Arrhenius plots was 1.1×10^{11} s^{-1}, which seems to be higher than the τ^{-1} values of the backbone motion. Thus, if one pays attention to one azochromophore molecule, free volume redistribution during the isomerization seems to be negligible at least for the redistribution due to the backbone motion. In contrast, the time scale of the isomerization measurement was far longer than that of the free volume redistribution, as seen from Figures 6, 9, and 10. This means that the state of the free volume distribution in the matrix changes constantly during the measurement. Thus, we considered that the average free volume (hole size) V_f in the matrix was concerned with the isomerization rate. If V_f is smaller than the average hole size required to allow the isomerization V_a, the isomerization reaction should be influenced by the increase in T_g. Since the PPO backbone, which rearranges during the time scale of the isomerization measurement, is linked to the azochromophores, the term of the average hole size was used. Consequently, V_f seems to be larger than V_a at this temperature range. The Arrhenius plots of the isomerization rate were thus expressed by a single straight line, independent of the $LiClO_4$ concentrations and the cross-linking densities.

Ion-Transport Process. Ion transport in a rubbery matrix also seems to proceed when a carrier ion finds a hole large enough to allow the ionic migration. The ionic conductivity measured is the bulk conductivity, which consists in the dc conductivity excluding the electrode processes. Thus, we should consider the average hole size for the ionic migration V_i. Similar to the isomerization process, if V_f is larger than V_i, the ionic conductivity should not be influenced by the T_g of the matrix. However, the ionic conductivity tended to decrease with increasing T_g, and its temperature dependence showed a WLF-type profile. This suggests that V_f is smaller than V_i. Thus, the ionic conductivity is influenced by the free volume redistribution due to the backbone motion. Although the volume of naked ions (Li^+ and ClO_4^- ions) is very small, V_i is led to be larger than V_a. We considered that the motion of the PPO backbone mediated the ionic transport in the PPO–$LiClO_4$ complexes.

A part of the incorporated $LiClO_4$ dissociates in the PPO network polymers via the interaction of the polar groups in the polymer backbone. The carrier ions in the complexes exist as solvated ions by the polar groups. The polymer segments with the associated ions constantly rearrange because the complexes are in a rubbery state. This rearrangement changes the local position of the carrier ions. The solvation by the other polymer segments dominates sometime after the change in the local position of the carrier ions, and then the segmental motion causes again the ionic migration. The repetition of the association of the carrier ions to the polymer segments, the segmental motion with the associated ions, and the dissociation from the polymer segments might cause the ionic transport in the PPO–$LiClO_4$ complexes. The segmental motion with the associated ions seems to be the rate-determining step for the ionic conduction. This consideration may be responsible for the analogy in the results of both ionic conductivity and dielectric relaxation time.

Registry No. 4,4′-$ClCOC_6H_4N{=}NC_6H_4COCl$, 10252-29-6; $ClCO(CH_2)_8COCl$, 111-19-3; propoxylated glycerol, 25791-96-2.

References and Notes

(1) Armand, M. B.; Chagagno, J. M.; Duclot, M. J. In *Fast Ion Transport in Solids*; Vashishta, P., Mundy, J. M., Shenoy, G. K., Eds.; North-Holland: Amsterdam, 1979; pp 131–136.
(2) Dupon, R.; Papke, B. L.; Ratner, M. A.; Whitmore, D. H.; Shriver, D. F. *J. Am. Chem. Soc.* **1982**, *104*, 6247.
(3) Killis, A.; LeNest, J. F.; Cheradame, H.; Gandini, A. *Makromol. Chem.* **1982**, *183*, 2835.
(4) Watanabe, M.; Sanui, K.; Ogata, N.; Inoue, F.; Kobayashi T.; Ohtaki, Z. *Polym. J.* (*Tokyo*) **1984**, *16*, 711.
(5) Watanabe, M.; Sanui, K.; Ogata, N.; Kobayashi, T.; Ohtaki, Z. *J. Appl. Phys.* **1985**, *57*, 123.

(6) Watanabe, M.; Sanui, K.; Ogata, N.; Inoue, F.; Kobayashi, T.; Ohtaki, Z. *Polym. J.* (*Tokyo*) **1984**, *17*, 549.
(7) Watanabe, M.; Togo, M.; Sanui, K.; Ogata, N.; Kobayashi, T.; Ohtaki, Z. *Macromolecules* **1984**, *17*, 2908.
(8) Dupon, R.; Papke, B. L.; Ratner, M. A.; Shriver, D. F. *J. Electrochem. Soc.* **1984**, *131*, 586.
(9) Watanabe, M.; Rikukawa, M.; Sanui, K.; Ogata, N.; Kato, H.; Kobayashi, T.; Ohtaki, Z. *Macromolecules* **1984**, *17*, 2902.
(10) Blonsky, P. M.; Shriver, D. F.; Austin, P.; Allcock, H. R. *J. Am. Chem. Soc.* **1984**, *106*, 6854.
(11) Nagaoka, K.; Naruse, H.; Shinohara, I.; Watanabe, M. *J. Polym. Sci., Polym. Lett. Ed.* **1984**, *22*, 659.
(12) Chiang, C. K.; Davis, G. T.; Harding, C. A.; Takahashi, T. *Macromolecules* **1985**, *18*, 825.
(13) Sasabe, H.; Saito, S. *Polym. J.* (*Tokyo*) **1972**, *3*, 624.
(14) Miyamoto, T.; Shibayama, K. *J. Appl. Phys.* **1973**, *44*, 5372.
(15) Tomlinson, M. L. *J. Chem. Soc.* **1946**, 756.
(16) Ross, D. L.; Blanc, J. In *Techniques of Chemistry. Photochromism*; Brown, G. H., Ed.; Wiley: New York, 1971; Vol. III, Chapter V, pp 500–515.
(17) Lamarre, L.; Sung, C. S. P. *Macromolecules* **1983**, *16*, 1729.

Study of the Equilibrium and the Kinetics of the Fluorescence Enhancement on Mixing Solutions of Auramine O and Poly(methacrylic acid)

Yongcai Wang and Herbert Morawetz*

Department of Chemistry, Polytechnic University, Brooklyn, New York 11201.

Received March 3, 1986

ABSTRACT: The steady-state fluorescence of aqueous solutions containing poly(methacrylic acid) (PMA) and Auramine O (AO) was studied as a function of pH and the ratio of the PMA normality and the AO molarity (P/D) by viscosity, UV absorption, and emission intensity. The difference spectra of AO in the presence and absence of PMA were shifted by PMA addition at low P/D values but exhibited isosbestic points at high P/D. These difference spectra were interpreted in terms of the PMA–AO association constant K at pH 4.05, 4.98, and 6.02. The shape of these difference spectra was similar to the AO difference spectrum in 50% aqueous dioxane and water. Emission intensities of AO in PMA solutions at low ionic strength increased with pH as long as the PMA remained in its compact conformation but dropped sharply on PMA expansion. At an ionic strength of 0.2 M, the emission intensity decreased with increasing pH even before the polymer expansion. Estimates of K from the dependence of the emission intensity on P/D yielded at pH 4.05 a value similar to that derived from difference absorption spectra, but at pH 4.98 the K obtained from fluorescence data was 4 times smaller. The rise of AO emission intensity on substituting 50% dioxane for water was relatively small, so that the decrease in the polarity of the microenvironment can account for only a small portion of the fluorescence increase when AO is bound to the compact form of PMA. Stopped-flow experiments of the kinetics of fluorescence enhancement when AO solutions are mixed with solutions of PMA yielded rate constants that remained constant or decreased with increasing PMA concentration. This indicates that the fluorescence increase is due to a conformational transition following PMA–AO association. The final approach to equilibrium has the unexpectedly low rate constant of 0.1 s^{-1}.

Introduction

In 1954 Oster discovered[1] that Auramine O, bis(4-(dimethylamino)phenyl)methylideneammonium chloride (AO), which fluoresces very weakly in water solution, has its emission intensity dramatically increased in the presence of DNA. Four years later, he reported[2] a similar effect in the presence of poly(methacrylic acid) (PMA). He suspected that the phenomenon was due to the local rigidity of the medium which would prevent the quenching of the excited molecule by internal rotation and showed that the emission intensity of AO increased, in fact, with the viscosity of its solutions.[3]

The change in the fluorescence intensity of AO when associated with PMA is of special interest because this polymeric acid exhibits a cooperative transition from a highly contracted to an expanded state at a critical density of anionic charges along the chain molecule.[4] Anufrieva et al.[5] showed that the enhancement of the AO fluorescence is associated with the contracted form of PMA—thus, the effect disappears when this form is destabilized by a high degree of ionization, α, of the PMA or when addition of methanol to the aqueous solution eliminates the hydrophobic bonds opposing chain expansion. Anufrieva et al. believed that only the contracted form of PMA binds AO and that the fluorescence intensity of the dye is proportional to its amount complexed with the polymer.

An extensive and careful study in Mandel's laboratory[6] showed that the situation is, in fact, much more complex. Comparing the fluorescence data with the results of dialysis equilibria of AO and PMA at varying degrees of ionization, they concluded that the binding of AO increases monotonously with the PMA charge density, even though the fluorescence intensity may drop precipitously in the range of α corresponding to the transition from the compact to the expanded state of the polymer. This drop of emission intensity was very pronounced when the ratio of the polymer normality to the molarity of the dye, P/D, was very high, while for $P/D \leq 2$ the fluorescence varied only slightly with α, with the maximum shifting to high α values. Thus, the fluorescence was shown to depend not only on the amount of the dye complexed with the polymer but also on the expansion of the polymer chain and the fraction of the PMA residues associated with the dye. Another striking observation, based on titration and viscosity behavior, was the stabilization of the compact PMA form by minute amounts of AO.

A few years ago, Chen and Thomas[7] showed that the emission intensity from a solution containing PMA and pyrene changes sharply when the polymer expands and they used a stopped-flow apparatus with fluorescence